HHS Public Access

Author manuscript

Adv Ther (Weinh). Author manuscript; available in PMC 2022 May 01.

Published in final edited form as:

Adv Ther (Weinh). 2021 May ; 4(5): . doi:10.1002/adtp.202000278.

Near-infrared Fluorophores for Thrombosis Diagnosis and Therapy

Bin Sun,

Joint Laboratory of Opto-Functional Theranostics in Medicine and Chemistry, The First Hospital of Jilin University, Changchun, 130061, P.R. China; State Key Laboratory of Supramolecular Structure and Materials, College of Chemistry, Jilin University, Changchun 130012, P.R. China

Kenneth S. Hettie,

Molecular Imaging Program at Stanford (MIPS), Department of Radiology, Stanford University School of Medicine, Stanford, California 94305, United States

Shoujun Zhu

Joint Laboratory of Opto-Functional Theranostics in Medicine and Chemistry, The First Hospital of Jilin University, Changchun, 130061, P.R. China; State Key Laboratory of Supramolecular Structure and Materials, College of Chemistry, Jilin University, Changchun 130012, P.R. China

Abstract

Thrombosis is an adverse physiological event wherein the resulting thrombus and thrombus-induced diseases collectively result in high morbidity and mortality rates. Currently, nano-medicines that incorporate fluorophores emitting in the near-infrared-I (NIR-I, 700-900 nm) spectral region into their systems have been adopted to afford thrombosis theranostics. However, several unsolved problems such as limited penetration depth and image quality severely impede further applications of such nano-medicine systems. Fortunately, the ability to incorporate fluorophores emitting in the NIR-II (1000-1700 nm) window into nano-medicine systems can unambiguously identify biological processes with high signal-to-noise, deep tissue penetration depth, and high image resolution. Considering the inherently favorable properties of NIR-II fluorophores, we believe such have enormous potential to quickly become incorporated into nano-medicine systems for thrombosis theranostics. In this review, we i) discuss the development of NIR fluorescence as an imaging modality and fluorescent agents; ii) comprehensively summarize the recent development of NIR-I fluorophore-based nano-medicine systems for thrombosis theranostics; iii) highlight the state-of-the-art NIR-II fluorophores that have been designed for the specific purpose of affording thrombotic diagnosis; iv) speculate on possible forward avenues for the use of NIR-II fluorophores towards thrombosis diagnosis and therapy; and v) discuss the potential for their clinical translation.

Graphical Abstract

Near-infrared bioimaging provides a vital tool for understanding physiological and pathological processes in living organisms, particular in the emerging NIR-II window with much improved imaging quality. Since thrombosis and thrombus-related diseases seriously affect human health,

khettie@stanford.edu.

this review comprehensively summarizes NIR-I fluorophore-based nano-medicine and discusses the attractive state-of-the-art NIR-II theranostic systems for thrombosis diagnosis and therapy.

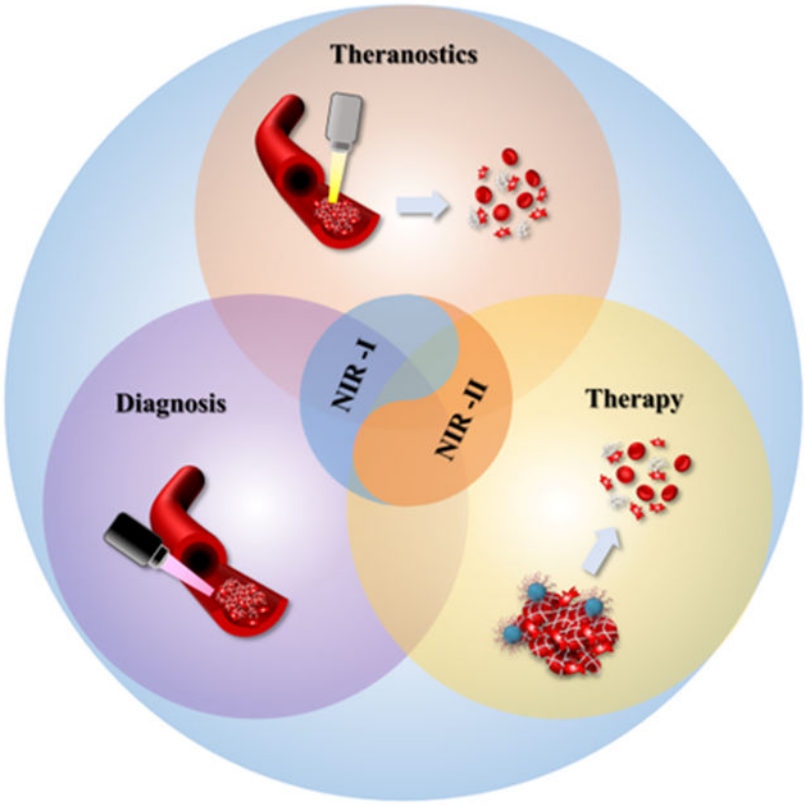

Keywords

Near-infrared fluorophores; thrombus-related diseases; diagnosis; therapy

1. Introduction

Thrombosis is an acute pathological event that rapidly evolves into numerous fatal cardia-cerebrovascular diseases such as coronary heart disease, ischemic stroke, pulmonary embolism, and deep vein thromboembolism.[1] Moreover, recent literature has reported that thrombosis or thrombus-induced diseases (e.g., pulmonary embolism) are closely associated with virulent novel coronavirus 2019 diseases (COVID-19), wherein patients infected with COVID-19 would have greater susceptibility to becoming afflicted with thrombotic disease(s) and would entail prolonged recovery from COVID-19.[2] As such, considerable attention has been attracted towards exploring the pathogenesis of thrombus-induced diseases as well as finding highly-effective theranostic strategies to diagnose and treat patients, both of which would help decrease the high morbidity and mortality rates.

Thrombi (i.e., blood clots) are classified as either arterial thrombi or venous thrombi, wherein both are triggered by highly-complex pathogenesis. Accordingly, gaining a complete understanding of the thrombus-related pathogenic processes would have enormous

significance in the development of new theranostic strategies for aiding patients afflicted by such. Platelets, fibrin, thrombin, and innate immune cells are collectively the major participants in thrombus formation.[3] Once blood vessels are damaged, the platelets actively aggregate around the injured sites, whereby the platelets are the main elements of the formed thrombus. Meanwhile, the injured vessel wall could expose collagen and tissue factor(s) to the circulating blood. The exposed collagen prompts the activation and aggregation of circumjacent platelets. The circulating tissue factor(s) give rise to thrombin formation that could initiate the activation of platelets and formation of fibrin, which is also a primary component of the formed thrombus.[4] In clinic, traditional imaging modalities, such as magnetic resonance imaging (MRI) and computed tomography (CT), are only appropriate for detecting previously-discovered thrombi. Moreover, such modalities relay information that reports on only the morphological features of thrombi, and thus they neither afford real-time detection nor discernment of its pathological state, both of which are necessary for urgently treating thrombus-induced diseases. NIR fluorescence imaging is an advanced detection technology that provides real-time visualization for immediate diagnosis, unambiguous feedback on anatomical structure information, no exposure to radiation, and high sensitivity. As a result of its characteristics and capabilities, NIR fluorescence imaging has developed into a remarkable detection modality for fundamental and clinical diagnostic research.[5]

The fatal effects of thrombus-induced diseases have strongly encouraged researchers to explore various new theranostic strategies. Nano-medicines hold considerable potential in allowing for the diagnosis and treatment of diseases because of nano-medicines could overcome commonly-encountered clinical challenges, such as not affording side reaction(s), not being invasive, and not requiring high dosage.[6] In addition, nano-medicines can manage rational release of therapeutic drugs via allowing for targeted delivery, which improves their therapeutic capacity as a result of their ability to decrease drug-loss while circulating in blood.[6a, 7] Some nano-medicines have rapidly evolved into allowing for probing thrombotic progress and treatment of thrombus-related diseases.[8] To do so, fluorescence imaging and fluorophores that emit in the NIR optical window have been implemented. The NIR optical window (700-1700 nm) can be segregated into NIR-I spectral region (700-1000 nm) and the NIR-II spectral region (1000-1700 nm). Numerous theranostic-based strategies that have been developed make use of NIR-I fluorophores to accomplish early detection and effective treatment of thrombus-related diseases. As a result, researchers have committed considerable efforts towards advancing nano-medicines that have the capabilities of facilitating *in vivo* imaging for diagnostic detection and targeted drug delivery for therapeutic treatment.

Accordingly, here we orient the contents of this review towards i) covering the advancing developments of NIR fluorophores and emphasizing the merits of using NIR-II fluorophores for bioimaging application, especially for the visualization, diagnosis, and treatment of thrombus-related diseases; ii) comprehensively summarizing the recent development of cutting-edge NIR-I fluorophore-based theranostic systems towards thrombus-related diseases; iii) highlighting the state-of-the-art NIR-II fluorophores that can be utilized for the diagnosis and/or treatment of the aforementioned; and iv) discussing the potential for their clinical translation. In addition, we call attention to the key direction(s) towards which the

development of NIR-II fluorophores for thrombotic diagnosis and therapy is heading and its significance.

2. Near-infrared fluorescence imaging

Optical bioimaging plays a key role in the clinical diagnosis and treatment of various diseases.[5c, 9] As a result of affording real-time visualization of anatomical structures and the surgical environmenSt, fluorescence image in the NIR-I spectral region has become broadly adopted for disease detection and imaging-guided surgery. However, intravital imaging quality spanning the entire optical window is impaired by the interaction between photons and biological tissues (i.e., light absorption and photon scattering), which is responsible for the extent emitted fluorescence light penetrates tissue (Figure 1a,b).[10] Thus, numerous efforts taking place currently focus on i) the creation of fluorescent contrast agents with maximal light penetration depth; and ii) the exploration of innovative imaging instrumentation demonstrating high sensitivity towards the detection of photons.[11] As a result of the ability to image deeper into biological material, these fluorophores that emit light in the NIR fluorescence window have emerged for using in biomedical applications. Particularly, noninvasive imaging in the NIR-II spectral region provides higher image quality when compared with doing so in the NIR-I spectral region because of significantly reduced adverse effects between photons and tissues (Figure 1c,d).[10, 11a] Thus, NIR-II fluorescence imaging technology provides a vital platform for achieving insight into the behavior of biological materials and processes such as anatomical structure and *in vivo* metabolic pathway. Currently, fluorophores that allow for imaging in the NIR-II window have been widely utilized for tumor detection and image-guided surgery in animals by following their whole-body blood circulation and/or targeting to tumor sites. However, for thrombosis imaging, only inherent blood circulation could transport NIR-II fluorophores to the thrombotic sites that make NIR-II imaging for thrombosis diagnosis have enormous potential for clinical translation and custom-tailored applications.

3. NIR-II fluorophores

Emerging fluorescence imaging technology in the NIR-II spectral region would provide an important tool for i) noninvasively exploring biological processes and discerning new biological information; and ii) diagnostics and therapeutics in both basic research and clinical practice. Recently-developed fluorophores that emit in the NIR-II spectral region could significantly improve the resolution quality of fluorescence imaging to help provide new information in basic research and clinicl practice. Thus, the pursuit of developing high-performance fluorescent materials is the primary direction for NIR-II imaging. In sync with their evolutionary pathway, various classes of NIR-II fluorescent materials have been developed via using rational design and engineering along with sophisticated chemical synthesis: single-walled carbon nanotubes (SWCNTs),[12] quantum dots (QDs),[13] rare earth-doped nanoparticles (RENPs),[14] semiconducting polymer-based nanoparticles (SPNPs),[15] organic small-molecule dyes (SMDs),[16] and aggregation-induced emission luminogens (AIEgens)[17] (Figure 2).

3.1 Inorganic fluorophores

Dai et al. progressed as a pioneer in fluorescence imaging by achieving intravital fluorescence imaging in the NIR-II optical window with the aid of an inorganic fluorescent agent, a SWCNT.[12a] This work attracted widespread attention and marked the beginning of fluorescence imaging within the NIR-II optical window in biological tissue. Subsequently, SWCNTs, QDs with higher quantum yield, and RENPs that have a tunable emission wavelength, were utilized for i) imaging the blood vasculature; ii) detecting tumor and lymph nodes; and iii) image-guided surgery by implementing fluorophores that emit light in the NIR-II spectral region.[18] Image-guided surgery for metastatic ovarian cancer has been achieved by using rare-earth down-conversion nanoparticles (DCNP) with emission wavelength within the NIR-II window. Specifically traveling to tumor and stable tumor retention allowed for superior tumor-to-normal tissue (T/NT) imaging and its precise image-guided resection.[18c] Shortly thereafter, Wang *et al.* reported an activatable nanotheranostic system (FEAD1) based on Ag_2S quantum dots and anticancer drug doxorubicin (DOX) to perform in sync peritoneal metastasis tumor diagnosis and therapy. Tumor microenvironment-activated NIR-II imaging and responsive DOX releasing strategy opened an innovative method to tumor theranostic.[19] The biomedical applications of these inorganic fluorescent materials have gained immense interest. However, the i) biosafety concern and potential toxicity caused by long-term retention in the reticuloendothelial system (RES); and ii) slow metabolism restrict the clinical translation of these inorganic materials. Fortunately, emerging SMDs that emit in the NIR-II optical window with favorable biosafety and biocompability bring new opportunity for intravital imaging.

3.2 Organic small-molecular dyes

SMDs have received unprecedented attention in recent years owing to the ability to i) control their molecular structures; ii) tune their emission wavelength that can span the entire NIR optical window; iii) low biotoxicity; iv) excellent biocompatibility; and v) rapid excretion. In particular, the Food and Drug Administration (FDA) has approved the commercial organic small-molecular dyes, indocyanine green (ICG) and IRDye® 800CW, for using in clinical trials.[20] Methylene blue (MB), another commercial organic dye, has also received approval by the FDA for using in image-guided surgery in a clinical setting.[21] However, the absorption and emission channel of all of the aforementioned dyes are in the NIR-I spectral region, and thereby makes it difficult to explore and visualize deeper tissue structures and biological phenomena. Accordingly, absorption and fluorescence emission in the NIR-I spectral region affords restricted use in clinical applications. The breakthrough regarding small-molecule dye that emit wavelength stretching from the NIR-I spectral region into the NIR-II spectral region was accomplished by Dai et al. in 2015.[16a] In his seminal work, a donor-acceptor-donor (D-A-D) structure-based NIR-II fluorophore, CH1055, decorated with PEG, was prepared and used for *in vivo* targeted brain tumor imaging, wherein it provided high renal excretion due to its enhanced water solubility (~90% excreted through the kidneys within 24 h). A series of SMDs were developed following the emergence of PEGylated CH1055. Up until then, the SMDs primarily derived from basic D-A-D structure or polymethine backbone (i.e., cyanine dyes).[16b] The essential physical and photophysical properties of small-molecule organic NIR-II dyes are i) high brightness (which depends on the quantum yield (φ) and extinction coefficient (ε)); ii) suitable photostability; iii)

absorption/emission wavelengths in NIR-II region; iv) satisfactory water-solubility; and v) excellent biocompatibility. Numerous innovative works are ongoing in the pursuit of the above-mentioned characteristics in a SMD for using in the NIR-II spectral region. For a more comprehensive understanding of NIR-II fluorescent dyes, such as modified strategy and chemical synthesis principle, readers can refer to previous reviews.[16b, 22] In comparison to inorganic NIR-II fluorophores, SMDs that possess high metabolic rates, low biotoxicity, and stable structure make them more suitable for performing intravital imaging. Given such merits, we believe that NIR-II SMDs have great application and clinical translation potential for detecting, diagnosing, and treating thrombosis and thrombus-related diseases.

4. NIR bioimaging for thrombosis diagnosis and therapy

Capitalizing on the abilities of high-performance NIR-II fluorescence agents, anatomical structure and diagnostic information can be exceptionally outlined by bioimaging in the NIR-II spectral region which affords excellent transparency. However, the cutting-edge NIR-II imaging technology has been rarely utilized for thrombosis detection. Fortunately, NIR-I bioimaging has gradually evolved into serving the role of an instrumental supporting modality for thrombosis treatment.[23] In particular, advancing NIR-I image-aided theranostic systems would lay the foundation for and push the development for NIR-II imaging towards such.

4.1 NIR-I imaging

Nano-medicines have been deemed a milestone of innovation in relation to the development of diagnostics and therapeutics.[24] In recent years, nano-medicines have rapidly evolved towards the use of NIR fluorophores for strategies for thrombosis and thrombus-induced disease detection and treatment. Currently, such nano-medicines primarily utilize one or two fluorophores that emit light in the NIR-I optical window for diagnostic purposes only, or use in a concerted fashion to both diagnose and treat thrombosis and thrombus-induced diseases, respectively. Among many platforms, artificial nanoparticles are the major carrier of NIR-I fluorophores that are leading to the realization of thrombosis detection and/or thrombus-induced disease interventions. Compared with the MRI and CT diagnosis strategies, NIR-I fluorescence imaging affords real-time imaging and has the flexibility to present more detailed information regarding the biological processes underlying thrombosis.[23a, 25] Thus, NIR-I fluorophores usually act as i) a scout in nano-systems so as to precisely identify thrombus lesions; and ii) an indicator capable of revealing the effects of therapeutic treatment. As important tools, NIR-I fluorophores usually cater to various nanoparticles by bioconjugation or chemical synthetic strategies.[23a, b, 26]

Kang et al. reported a multifunctional theranostic system for targeted imaging of thrombus and prevention of new thrombus formation. The NIR-I dye, IR-820, was synthetically prepared and conjugated to the backbone of a polymer chain, named FTIAN, which consisted of boronated antioxidant polymers and fibrin-targeting lipopeptides. The nanoparticles that formed by the self-assembly of the FTIAN polymer could identify blood clots by recognizing fibrin. Followingly, the administration and delivery of an antiplatelet

drug and the depletion of hydrogen peroxide (H_2O_2) ultimately prevented platelet aggregation in ferric chloride ($FeCl_3$)-induced carotid thrombosis (Figure 3a,b). Thus, the fluorophore, IR-820, afforded the real-time imaging of FTIAN travel to and accumulation at thrombus sites (Figure 3c,d).[23a]

Following this report, a responsive fluorescent nanoparticle for thrombotic diagnosis and therapy was reported by Kwon et al. The commonly-used cyanine dye, Cy5.5, served as a fluorescent imaging probe, which was then conjugated to thrombin-activatable peptide by a simple amidation reaction between amine functional moiety (-NH_2) and *N*-hyrdroxysuccinimide (NHS) to construct an "OFF-ON" fluorescent peptide, as shown in figure 4a. The nanoparticles coated with activable fluorescent peptide had no fluorescence emission in aqueous solution due to the quenching effect upon their aggregation. Once the aggregated nanoparticles were cleaved by thrombin, which existed around only thrombotic sites, the fluorescence emission of Cy5.5 was triggered from an "OFF" state to an "ON" state for the purpose of imaging thrombus. Interestingly, the fluorescence intensity increased ~ 30-fold after cultured with thrombin *in vitro* (Figure 4).[23b]

Recently, some biomimetic nano-medicine systems have emerged for thrombosis therapy, which could rapidly target thrombotic sites, deliver thrombolytic agents, and reduce risk of thrombus-induced complications.[27] Gong et al. constructed multifunctionally biomimetic nanoparticles (T-RBC-DTC) that could i) target thrombotic regions for the delivery of the antithrombotic drug, named tirofiban; and ii) downregulate overproduced H_2O_2 in $FeCl_3$-induced carotid artery thrombosis model. A biomimetic red blood cell membrane modified with fibrin-targeting peptide served as a coating to chaperone the drug-loaded dextran nanocore for obtaining thrombosis therapy nanoparticle shown in figure 5a.[27a] Regrettably, in this work, Cy5.5 dyes that emitted in the NIR-I spectral region were administrated to detect the thrombolytic level as shown figure 5b.[27a] The lower resolution of images caused by light scattering and autofluorescence potentially could be improved by utilizing NIR-II fluorophores, such as LZ-1105 polymethine dyes that were reported by Zhang et al.[28]

In the last few years, we witnessed a rapid increase in utilizing NIR-I fluorophores as vital ingredients of nano-medicines for diagnosis thrombosis and/or feedback therapeutic information. Due to the advantages of using a NIR-I fluorophore (as opposed to not using a fluorophore), an abundant amount of research results were obtained: i) the NIR-I fluorophores as nanoprobe could precisely report on thrombus formation or damaged vessel sites with real-time transmission of biological information; and ii) the existing NIR-I fluorophores readily conjugate to multifunctional thernostic systems. However, some long-standing challenges remain. Ambiguous imaging capability and limited tissue penetration depth make NIR-I fluorophore-aided nano-medicines uncapable of affording the diagnosis of complex thrombus-induced diseases. For example, for ischemic stroke, the complex pathological environment and skull barrier would allow fluorophores with excellent photostability, great brightness, and deeper penetration depth to collect accurate information from the disease microenvironment.[29] Moreover, an ultrashort treatment window due to unpredictable morbidity is the key consideration for ischemic stroke therapy. The real-time feedback capacity of NIR-II imaging could both quickly locate the diseased sites and assist image-guided endovascular thrombectomy in a timely manner. The thrombus detachment

and its migration from deep vein to lung in the marching surgery and postoperative recovery is an unavoidable event which, if otherwise, would improve mortality rates that result from the surgical process and the difficulty of postoperative recovery. In clinic, CT angiography is utilized for the diagnosis and real-time detection of embolism-transfer induced pulmonary embolism via injecting an iodic contrast agent into the patient. The great time-consumption and toxicity of iodine could bring huge disaster for patients. Thus, we anticipate nano-medicines, which combine superior NIR-II fluorescent agents and thrombolytic agents, could overcome this issue by unambiguously imaging the floating thromboembolus, and rapidly destroying the thrombus focus.

4.2 NIR-II imaging

Although various multifunctional nano-medicine systems based on NIR-I fluorophores have been developed for diagnosis and therapy of thrombosis, challenges remain for the detection and diagnosis of acute thrombus-induced diseases. Time-consuming detection technology (e.g., CT and MRI), biological tissue scatter the detected signal, and low quality image seriously dock the efficient therapy windows. Complicated biological behaviors around diseased microenvironment such as neural and cellular changes urge the development of highly-sensitive probes. For such challenges, NIR fluorescence imaging in the NIR-II spectral region can afford the ability to overcome such obstacles by exhibiting high spatiotemporal resolution, high signal-to-noise, deep light penetration depth and high sensitivity. As such, imaging in the NIR-II spectral region can allow for precisely discriminating thrombotic sites, the thrombotic microenvironment, and real-time tracing of thrombus fragment-generated embolus, all of which would merit considerable attention for potential clinical translation. However, there is scant information in the literature that utilize fluorophores with fluorescence emission in the NIR-II spectral region for the purpose of complex thrombus-induced diseases diagnosis and treatment.

Nevertheless, NIR-II fluorescence imaging technology has been widely used for angiography that afforded visualization of the vascular structure and provided hemodynamics information (Table 1). The unambiguous whole body and partial femoral artery structure with improved resolution and signal-to-background were imaged by using SWNTs and PbS/CdS as contrast agents, which both emit in the NIR-II optical window (Figure 6).[30]

A series of intravital vessel behavior revealed by these fluoroscent materials provided an inspiration for vascular disease diagnosis by using fluorescence imaging in the NIR-II optical window. Recently, Zhang et.al reported a water-soluble LZ1105 small-molecule fluorophore with a terminal diindole and four sulfonate groups which exhibited both adsorption and emission in the NIR-II optical region as well as superior water solubility (Figure 7a,b). Noninvasive monitoring of vascular environment changes were performed by using LZ1105 with high resolution and signal-to-background. LZ1105 underwent systemic administration by tail vein injection to afford real-time imaging of ischemic reperfusion and thrombolysis progress triggered by recombinant tissue plasminogen activator (rt-PA) in thrombosis murine models. The ischemic reperfusion level with different clipping period

and blood reflow after thrombolysis provided unambiguous feedback with satisfactory brightness (Figure 7c–f).[28]

Sun et al. reported a cRGD-decorated fluorescent dye that had peak emission at 1015 nm for using in *in vitro* and *in vivo* thrombosis diagnosis. The targeted organic dyes could distinguish early thrombus and old thrombus.[43] The organic NIR-II fluorophores have numerous advantages for *in vivo* and *in vitro* thrombosis or thrombus-related diseases diagnosis. However, there is very limited literature available on thrombus-induced diseases diagnosis via using NIR-II fluorophores. Such possibly attributes to some mistaken ideas: i) thrombus formation is a vascular disease that can be simply diagnosed by vessel imaging; ii) uncomplicated pathogenesis (platelets aggregation and fibrin network formation) reduces the attention towards thrombus-induced diseases; and iii) thrombus-related complications (embolism formation from deciduous thrombus) are neglected all the time. Aside from SMDs, other fluorophores such as SPNPs[36] also have emerged to image thrombus *in vivo,* with the rapid development of imaging in the NIR-II optical window. For example, a semiconducting polymer with high NIR-II brightness (PTQ) was used to prepare SPNPs, referred to as L1057. An image that unambiguously identified cerebral ischemia stroke was obtained using L1057 within the cranial window. Compared to ICG, the deep vascular structure was successfully imaged clearly due to the deep-tissue penetration of fluorescence emitted by L1057.[36]

Thrombosis diagnosis via utilizing optical imaging in the NIR-II optical window is gradually developing by numerous ongoing efforts. However, the thrombus-related disease therapy that is based on NIR-II imaging as administrated by nano-medicines aided with NIR-I imaging are rarely published. Whereas, the NIR-II imaging assisting nano-medicines, which integrated both diagnostics and therapeutics, have been widely used to combat tumors and cancer.[44] The benefits from these unique optical characteristics include deep tissue penetration depth, high temporal-spatial resolution, and improved signal-to-noise, NIR-II fluorophores can be qualified to support theranostic agents for simultaneous diagnosis and therapy of thrombus-releated diseases by apace confirming thrombus formation sites, providing more detailed pathological information, timely monitoring of microenvironmental changes, and accurately evaluating the therapeutic level. We believe that the conjugation of NIR-II fluorescence imaging with nano-medicines should open the way to new biomedical applications with regards to thrombosis and thrombus-related diseases diagnosis and therapy.

5. Mouse thrombosis and thrombus-related diseases model

Animal disease model construction is an extremely important bridge between lab research and clinical translation. Thrombosis and thrombus-related disease models constructed in living organisms play another vital role for evaluation of theranostic systems and in-depth understanding of thrombotic pathological and physiological information. Thanks to previous efforts, some mature animal thrombosis models have been constructed (Table 2).

Most typical, a $FeCl_3$-induced thrombosis model is prepared from venous or arterial vessels by coating with a certain concentration of $FeCl_3$ solution within a period of time to damage endothelial cell and induce platelet activation and aggregation.[47] This model is a basic tool

to evaluate thrombolytic or anticoagulant capacity of theranostic systems. Middle cerebral artery occlusion (MACO), another important thrombosis model, can evolve into cerebral ischemic stroke, which is a major cause of death worldwide. The lateral carotid artery is exposed by incising the lateral neck with its external branch ligated. After that, surgical nylon is inserted from the carotid bifurcation to occlude the middle cerebral artery (MCA). After a period of time, the surgical nylon is withdrawn to allow for ischemic reperfusion.[48] Apart from these typical thrombus-related models, a pulmonary embolism mouse model and an arteriovenous shunt thrombosis rat model were constructed to evaluate the therapeutic systems as part of fundamental research.[8a] The pulmonary embolism mouse model is conveniently acquired by tail-vein injection with thromboplastin and fibrinogen, each of which can trigger the formation of micro emboli. The formed micro emboli travel to the lung by circulating in the blood and give rise to the formation of pulmonary embolism.[49]

In vitro thrombosis models are simple and convenient tools for real-time feedback of the therapeutic process compared to *in vivo* models. The artificial thrombus formed by fresh blood agglomeration with the help of calcium chloride ($CaCl_2$) and thrombin has been utilized for intuitive evaluation of thrombolysis ability *in vitro*.[25, 45] Capillary thrombus and tail bleeding assay are also important in *in vitro* models for evaluating theranostic systems.[46] Thus, the active exploration of newly-fashioned thrombus-related disease murine models, such as mimetic thrombus detachment and migration, is another important avenue to push the clinical translation of fundamental research.

6. Conclusion and outlook

Near-infrared fluorescence imaging is an innovative modality for disease diagnosis and treatment. Due to low tissue autofluorescence and reduced photon scattering, NIR fluorescence imaging using fluorophores that have considerable brightness afford high-fidelity imaging and support prominent theranostic strategies for thrombus-related diseases. However, for select thrombus-induced diseases, such as acute ischemic stroke and pulmonary embolism, they exhibit a highly-complex physiological and pathological process that require urgent attention with fluorophores that emit in the NIR-II spectral region in order to achieve deeper insight into anatomical structures and obtain more detailed physiological and pathological information. Thus, some challenges are remaining and need to be overcome.

1. Currently, some fluorescent probes with emission wavelength in the NIR-II optical window have been established for intravital thrombus imaging and therapy. However, satisfactory NIR-II fluorophores with superior optical and biological characteristics are limited. Thus, more and more attention must be focused on high-performance fluorophore design from a molecular engineering point of view. Typical NIR-II fluorophores, D-A-D, polymethine and other dye types, with controllable chemical structures, provide an opportunity to obtain the desired fluorophores. Not only organic synthesis approaches, protein-chaperon strategies have improved brightness through protein-dye interaction.[16c, d] In particular, some NIR-I fluorophores reveal long emission tails that stretch into the NIR-II region. Based on this point, a novel strategy to improve optical and

biological characteristics of NIR-I fluorescent probes have emerged by coating fluorophore with protein that make NIR-I fluorophores emission in the NIR-II widow with enhanced brightness, alongside improved pharmacokinetics.[16e] In particular, rich functional groups of protein can be conjugated with biomarkers to target diseased tissues. This convenient chaperone strategy can serve as a special tool for thrombus-related diseases imaging and therapy.

2. Nano-medicine systems are believed to be an efficient and suitable theranostic platform for thrombus-related diseases due to such unique characteristics like precise aggregation to thrombus formation sites, designed particle size, and low biotoxicity. The artificial nanoparticles that incorporate NIR fluorophores emitting in the NIR-I optical window provide a direct path for the use of fluorophores that emit in the NIR-II spectral region for the diagnosis and therapy of thrombosis. Combining targeted nanoparticles with NIR-II fluorophores would allow for the tracing of pathway of the post-administrated nanoparticles *in vivo* and timely reveal the therapeutic information by real-time imaging. For complex thrombus-related diseases, the directed accumulation at thrombus formation sites and thrombus-induced injury regions is a prerequisite. Excellent targeted capacity can build up the diagnostic and therapeutic efficiency of nanoparticles by increasing the high-effective drug concentration around the diseased sites. Thus, researchers need to place efforts on exploring efficient designs of nano-medicine systems incorporating fluorophores that emit in the NIR-II spectral region.

3. *In vitro* diagnosis (IVD) strategy, is an important tool for noninvasive, rapid, and highly-sensitive disease diagnosis in clinical and fundamental research.[50] In both clinical and fundamental research, the development of *in vitro* thrombotic diagnosis is hindered by limited detectable biomarkers that only exist in thrombotic regions and rarely travel following with blood. The high sensitivity of NIR-II fluorescence imaging has obtained fruitful harvest in the field of disease diagnosis and therapy. Capitalizing on the prosperity of NIR-II probes and imaging systems, we anticipate that NIR-II fluorescence imaging should grow into a powerful tool for *in vitro* thrombotic diagnosis due to its high-sensitivity. The NIR-II fluorescent probes could be competent to pro-diagnose and monitor the complication in homecare of thrombus-related diseases due to activatable fluorescent signal and responsive fluorescent intensity.

4. However, some reasons responsible for limitations of the aforementioned to clinical translation include: i) complex chemical preparation and progress brings high cost and latent biotoxicity; ii) the biological distinctions between animal and person impede the clinical translation; and iii) the side-effects and toxicity in other organs are potential concerns. Thus, much more efforts should be made to overcome these obstacles and to propel NIR-II fluorophore-based theranostic nanosystems toward clinical application and evenly realize thrombus removal via implementing image-guided surgery.

Acknowledgements

This work was supported by Joint Laboratory of Opto-Functional Theranostics in Medicine and Chemistry, the First Hospital of Jilin University; and the Key Laboratory of Organ Regeneration & Transplantation of the Ministry of Education, the First Hospital of Jilin University and the Program of Assembly and Functionalities for Supramolecular Systems 2.0 (BP0618011). KSH's contribution to this work was supported, in part, by NIH/NCI fellowship: F32 CA213620.

Biographies

Bin Sun is a research associate in the First Hospital of Jilin University. He recived his M.S degree from joint program between State Key Laboratory of Polymer Physics and Chemistry, Changchun Institute of Applied chemistry, Chinese academy of sciences (CAS) and College of Chemistry and Materials Science, Liaoning Shihua University. His current research foucs on developing highly-effective theranostic systems based on NIR-II fluorophores for acute thrombus-related diseases visualization and therapy.

Kenneth S. Hettie received his Ph.D. from the University of Missouri-Columbia in 2014 under the supervision of Dr. Timothy E. Glass. After a one-year postdoctoral appointment in the laboratory of Dr. Eric T. Kool at Stanford University, he set forth on a 6-year postdoctoral appointment in the laboratory of Dr. Frederick T. Chin at Stanford University School of Medicine in the Department of Radiology, in part due to being awarded a 4-year NCI/NIH Ruth L. Kirschstein NRSA fellow (F32) award that he is currently fulfilling. He works on the development and implementation of targeted probes for the visualization of cancer-related biomarkers and functional events. He specializes in rational design, chemical synthesis, and analytical evaluation of sensors and probes.

Shoujun Zhu received his Ph.D. from Jilin University in 2014 under the supervision of Prof. Bai Yang and Junhu Zhang. After a two-year postdoctoral research period in the laboratory of Prof. Hongjie Dai at Stanford University, he further performed postdoctoral research with Dr. Xiaoyuan (Shawn) Chen at National Institute of Health (NIH) from 2017 to 2019. He joined Jilin University as a full professor in 2019. His research focuses on molecular fluorophores and intravital bioimaging. Shoujun Zhu has published over 100 papers that have been cited over 14000 times; he has an H-index 52 and has been selected as 2019-2020 "Highly Cited Researchers" by Clarivate Analytics.

References

[1]. a)Lippi G, Franchini M, Targher G, Nat. Rev. Cardiol 2011, 8, 502, 512 [PubMed: 21727917] b)Baglin T, Br. J. Haematol 2008, 141, 764. [PubMed: 18410449]

[2]. a)Bikdeli B, Madhavan MV, Jimenez D, Chuich T, Dreyfus I, Driggin E, Der Nigoghossian C, Ageno W, Madjid M, Guo YT, Tang LV, Hu Y, Giri J, Cushman M, Quere I, Dimakakos EP, Gibson CM, Lippi G, Favaloro EJ, Fareed J, Caprini JA, Tafur AJ, Burton JR, Francese DP, Wang EY, Falanga A, McLintock C, Hunt BJ, Spyropoulos AC, Barnes GD, Eikelboom JW, Weinberg I, Schulman S, Carrier M, Piazza G, Beckman JA, Steg G, Stone GW, Rosenkranz S, Goldhaber SZ, Parikh SA, Monreal M, Krumholz HM, Konstantinides SV, Weitz JI, Lip GYH, Global C-TC, Isth, Natf, Esvm, E. S. C. W. G. P. Ci, J. Am. Coll. Cardiol 2020, 75, 2950 [PubMed: 32311448] b)Wang T, Chen RC, Liu CL, Liang WH, Guan WJ, Tang RD, Tang CL, Zhang NF, Zhong NS, Li SY, Lancet Haematology. 2020, 7, 362.

[3]. Engelmann B, Massberg S, Nat. Rev. Immunol 2013, 13, 34. [PubMed: 23222502]

[4]. Furie B, Furie BC, N. Engl. J. Med 2008, 359, 938–949. [PubMed: 18753650]

[5]. a)Tian R, Ma H, Zhu S, Lau J, Ma R, Liu Y, Lin L, Chandra S, Wang S, Zhu X, Deng H, Niu G, Zhang M, Antaris AL, Hettie KS, Yang B, Liang Y, Chen X, Adv. Mater 2020, 32, 1907365b)Zhu S, Yung BC, Chandra S, Niu G, Antaris AL, Chen X, Theranostics. 2018, 8, 4141 [PubMed: 30128042] c)Hu Z, Fang C, Li B, Zhang Z, Cao C, Cai M, Su S, Sun X, Shi X, Li C, Zhou T, Zhang Y, Chi C, He P, Xia X, Chen Y, Gambhir SS, Cheng Z, Tian J, Nat. Biomed. Eng 2020, 4, 259. [PubMed: 31873212]

[6]. a)Chen G, Roy I, Yang C, Prasad PN, Chem. Rev 2016, 116, 2826 [PubMed: 26799741] b)van der Meel R, Sulheim E, Shi Y, Kiessling F, Mulder WJM, Lammers, Nat. Nanotechnol 2019, 14, 1007. [PubMed: 31695150]

[7]. Ma Y, Huang J, Song S, Chen H, Zhang Z, Small. 2016, 12, 4936. [PubMed: 27150247]

[8]. a)Zhao Z, Yang F, Zhang X, Sun J, He Z, Luo C, Biomaterials. 2020, 255, 120200 [PubMed: 32563945] b)Su M, Dai Q, Chen C, Zeng Y, Chu C, Liu G, Nano-Micro Lett. 2020, 12, 96.

[9]. Huang JG, Li JC, Lyu Y, Miao QQ, Pu K, Nat. Mater 2019, 18, 1133. [PubMed: 31133729]

[10]. He S, Song J, Qu J, Cheng Z, Chem. Soc. Rev 2018, 47, 4258. [PubMed: 29725670]

[11]. a)Hong GS, Antaris AL, Dai HJ, Nat. Biomed. Eng 2017, 1,0010b)Wang F, Wan H, Ma Z, Zhong Y, Sun Q, Tian Y, Qu L, Du H, Zhang M, Li L, Ma H, Luo J, Liang Y, Li WJ, Hong G, Liu L, Dai H, Nat. Methods 2019, 16, 545 [PubMed: 31086342] c)Zhu S, Herraiz S, Yue J, Zhang M, Wan H, Yang Q, Ma Z, Wang Y, He J, Antaris AL, Zhong Y, Diao S, Feng Y, Zhou Y, Yu K, Hong G, Liang Y, Hsueh AJ, Dai H, Adv. Mater 2018, 30, 1705799.

[12]. a)Welsher K, Liu Z, Sherlock SP, Robinson JT, Chen Z, Daranciang D, Dai H, Nat. Nanotechnol 2009, 4, 773 [PubMed: 19893526] b)Antaris AL, Robinson JT, Yaghi OK, Hong GS, Diao S, Luong R, Dai HJ, Acs Nano. 2013, 7, 3644 [PubMed: 23521224] c)Hong G, Diao S, Antaris AL, Dai H, Chem. Rev 2015, 115, 10816 [PubMed: 25997028] d)Dang X, Gu L, Qi J, Correa S, Zhang G, Belcher AM, Hammond PT, Proc. Natl. Acad. Sci. U. S. A., Early Ed 2016, 113, 5179.

[13]. a)Du Y, Xu B, Fu T, Cai M, Li F, Zhang Y, Wang Q, J. Am. Chem. Soc 2010, 132, 1470 [PubMed: 20078056] b)Hong G, Robinson JT, Zhang Y, Diao S, Antaris AL, Wang Q, Dai H, Angew. Chem., Int. Ed 2012, 51, 9818c)Bruns OT, Bischof TS, Harris DK, Franke D, Shi YX, Riedemann L, Bartelt A, Jaworski FB, Carr JA, Rowlands CJ, Wilson MWB, Chen O, Wei H, Hwang GW, Montana DM, Coropceanu I, Achorn OB, Kloepper J, Heeren J, So PTC, Fukumura D, Jensen KF, Jain RK, Bawendi MG, Nat. Biomed. Eng 2017, 1, 0056 [PubMed: 29119058] d)Franke D, Harris DK, Chen O, Bruns OT, Carr JA, Wilson MWB, Bawendi MG, Nat. Commun 2016, 7, 12749. [PubMed: 27834371]

[14]. a)Naczynski DJ, Tan MC, Zevon M, Wall B, Kohl J, Kulesa A, Chen S, Roth CM, Riman RE, Moghe PV, Nat. Commun 2013, 4, 2199 [PubMed: 23873342] b)Wang R, Li X, Zhou L, Zhang F, Angew. Chem. Int. Ed 2014, 53, 12086c)Zhong Y, Ma Z, Zhu S, Yue J, Zhang M, Antaris AL, Yuan J, Cui R, Wan H, Zhou Y, Wang W, Huang NF, Luo J, Hu Z, Dai H, Nat. Commun 2017, 8, 737 [PubMed: 28963467] d)Fan Y, Wang P, Lu Y, Wang R, Zhou L, Zheng X, Li X, Piper JA, Zhang F, Nat. Nanotechnol 2018, 13, 941. [PubMed: 30082923]

[15]. a)Hong GS, Zou YP, Antaris AL, Diao S, Wu D, Cheng, Zhang XD, Chen CX, Liu B, He YH, Wu JZ, Yuan J, Zhang B, Tao ZM, Fukunaga C, Dai HJ, Nat. Commun 2014, 5, 4206 [PubMed: 24947309] b)Huang JG, Xie C, Zhang XD, Jiang YY, Li JC, Fan QL, Pu KY, Angew. Chem. Int. Ed 2019, 58, 15120c)Lu X, Yuan P, Zhang W, Wu Q, Wang X, Zhao M, Sun P, Huang W, Fan Q, Polym. Chem 2018, 9, 3118.

[16]. a)Antaris AL, Chen H, Cheng K, Sun Y, Hong GS, Qu CR, Diao S, Deng ZX, Hu XM, Zhang B, Zhang XD, Yaghi OK, Alamparambil ZR, Hong XC, Cheng Z, Dai HJ, Nat Mater 2016, 15, 235 [PubMed: 26595119] b)Zhu S, Tian R, Antaris AL, Chen X, Dai H, Adv. Mater 2019, 31, 1900321c)Li B, Lu L, Zhao M, Lei Z, Zhang F, Angew. Chem., Int. Ed 2018, 57, 7483d)Antaris AL, Chen H, Diao S, Ma Z, Zhang Z, Zhu S, Wang J, Lozano AX, Fan Q, Chew L, Zhu M, Cheng K, Hong X, Dai H, Cheng Z, Nat. Commun 2017, 8, 15269 [PubMed: 28524850] e)Tian R, Zeng Q, Zhu S, Lau J, Chandra S, Ertsey R, Hettie KS, Teraphongphom T, Hu Z, Niu G, Kiesewetter DO, Sun H, Zhang X, Antaris AL, Brooks BR, Chen X, Sci. Adv 2019, 5, 0672.

[17]. a)Sheng Z, Guo B, Hu D, Xu S, Wu W, Liew WH, Yao K, Jiang J, Liu C, Zheng H, Liu B, Adv. Mater 2018, 30, 1800766b)Qi J, Sun C, Zebibula A, Zhang H, Kwok RTK, Zhao X, Xi W, Lam JWY, Qian J, Tang BZ, Adv. Mater 2018, 30, 1706856c)Xu Y, Li C, Xu R, Zhang N, Wang Z, Jing X, Yang Z, Dang D, Zhang P, Meng L, Chem. Sci 2020, 11, 8157.

[18]. a)Li CY, Zhang YJ, Wang M, Zhang Y, Chen GC, Li L, Wu DM, Wang QB, Biomaterials. 2014, 35, 393 [PubMed: 24135267] b)Ding F, Fan Y, Sun Y, Zhang F, Adv. Healthcare. Mater 2019, 8, 1900260c)Wang P, Fan Y, Lu L, Liu L, Fan L, Zhao M, Xie Y, Xu C, Zhang F, Nat. Commun 2018, 9, 2898. [PubMed: 30042434]

[19]. Ling SS, Yang XH, Li CY, Zhang YJ, Yang HC, Chen GC, Wang QB, Angew. Chem. Int. Ed 2020, 59, 7219–7223.

[20]. a)Vahrmeijer AL, Hutteman M, van der Vorst JR, van de Velde CJH, Frangioni JV, Nat. Rev. Clin. Oncol 2013, 10, 507 [PubMed: 23881033] b)Rosenthal EL, Warram JM, de Boer E, Chung TK, Korb ML, Brandwein-Gensler, Strong TV, Schmalbach CE, Morlandt AB, Agarwal, Hartman YE, Carroll WR, Richman JS, Clemons LK, Nabell LM, Zinn KR, Clin. Cancer Res 2015, 21, 3658. [PubMed: 25904751]

[21]. van Manen L, Handgraaf HJM, Diana M, Dijkstra J, Ishizawa T, Vahrmeijer AL, Mieog JSD, J. Surg. Oncol 2018, 118, 283. [PubMed: 29938401]

[22]. a)Zhang F, Lei Z, Angew. Chem., Int. Ed 2020, 10.1002/anie.202007040b)Cai Y, Wei Z, Song C, Tang C, Han W, Dong X, Chem. Soc. Rev 2019, 48, 22 [PubMed: 30444505] c)Ding F, Zhan Y, Lu X, Sun Y, Chem Sci. 2018, 9, 4370. [PubMed: 29896378]

[23]. a)Kang C, Gwon S, Song C, Kang PM, Park SC, Jeon J, Hwang DW, Lee D, Acs Nano. 2017, 11, 6194 [PubMed: 28481519] b)Kwon SP, Jeon S, Lee SH, Yoon HY, Ryu JH, Choi D, Kim JY, Kim J, Park JH, Kim DE, Kwon IC, Kim K, Ahn CH, Biomaterials. 2018, 150, 125 [PubMed: 29035738]) Lee J, Jeong L, Jung E, Ko C, Seon S, Noh J, Lee D, J. Controlled. Release 2019, 304, 164.

[24]. a)Li SP, Zhang YL, Ho SH, Li BZ, Wang MF, Deng XW, Yang N, Liu GN, Lu ZF, Xu JC, Shi QW, Han JY, Zhang LR, Wu Y, Zhao YL, Nie GJ, Nat. Biomed. Eng 2020, 4, 732 [PubMed: 32572197] b)Yang Y, Sun B, Zuo S, Li X, Zhou S, Li L, Luo C, Liu H, Cheng M, Wang Y, Wang S, He Z, Sun J, Sci. Adv 2020, 6, 1725.

[25]. Wan MM, Wang Q, Wang RL, Wu R, Li T, Fang D, Huang YY, Yu YQ, Fang LY, Wang XW, Zhang YH, Miao ZY, Zhao B, Wang FH, Mao C, Jiang Q, Xu XQ, Shi DQ, Sci. Adv 2020, 6, 9014.

[26]. Qiao RR, Huang XM, Qin Y, Li YH, Davis TP, Hagemeyer CE, Gao MY, Nanoscale. 2020, 12, 8040. [PubMed: 32239038]

[27]. a)Zhao Y, Xie R, Yodsanit N, Ye M, Wang Y, Gong S, Nano today. 2020, 35, 100986 [PubMed: 33072177] b)Xu JC, Zhang YL, Xu JQ, Liu GN, Di CZ, Zhao, Li X, Li Y, Pang NB, Yang CZ, Li YY, Li BZ, Lu ZF, Wang MF, Dai KS, Yan R, Li SP, Nie GJ, Adv. Mater 2020, 32, 1905145.

[28]. Li B, Zhao M, Feng L, Dou C, Ding S, Zhou G, Lu L, Zhang H, Chen F, Li X, Li G, Zhao S, Jiang C, Wang Y, Zhao D, Cheng Y, Zhang F, Nat. Commun 2020, 11, 3102. [PubMed: 32555157]

[29]. a)Alves HC, Treurniet KM, Jansen IGH, Yoo AJ, Dutra BG, Zhang G, Yo L, van Es ACGM, Emmer BJ, van den Berg R, van den Wijngaard IR, Nijeholt G. J. L. a., Vos J-A, Roos YBWEM, Schonewille W, Marquering HA, Majoie CBLM, Investigators MCR, Stroke. 2019, 50, 3156 [PubMed: 31597552] b)Lu Y, Li C, Chen Q, Liu P, Guo Q, Zhang Y, Chen X, Zhang Y, Zhou W, Liang D, Zhang Y, Sun T, Lu W, Jiang C, Adv. Mater 2019, 31, 1808316.

[30]. Ma Z, Zhang M, Yue J, Alcazar C, Zhong Y, Doyle TC, Dai H, Huang NF, Adv. Funct. Mater 2018, 28, 1803417. [PubMed: 31327961]

[31]. Hong G, Lee JC, Robinson JT, Raaz U, Xie L, Huang NF, Cooke JP, Dai H, Nat. Med 2012, 18, 1841. [PubMed: 23160236]

[32]. Diao S, Blackburn JL, Hong G, Antaris AL, Chang J, Wu JZ, Zhang B, Cheng K, Kuo CJ, Dai H, Angew. Chem., Int. Ed 2015, 54, 14758.

[33]. Li H, Wang X, Li X, Zeng S, Chen G, Chem. Mater 2020, 32, 3365.

[34]. Lian W, Tu D, Hu P, Song X, Chen X, Nano Today. 2020, 35, 100943.

[35]. Guo B, Feng Z, Hu D, Xu S, Middha E, Pan Y, Liu C, Zheng H, Qian J, Sheng Z, Liu B, Adv. Mater 2019, 31, 1902504.

[36]. Yang YQ, Fan XX, Li L, Yang YM, Nuernisha A, Xue DW, He C, Qian J, Hu QL, Chen H, Liu J, Huang W, Acs Nano. 2020, 14, 2509. [PubMed: 32022539]

[37]. Liu S, Chen C, Li Y, Zhang H, Liu J, Wang R, Wong STH, Lam JWY, Ding D, Tang BZ, Adv. Funct. Mater 2020, 30, 1908125.

[38]. Lin J, Zeng X, Xiao Y, Tang L, Nong J, Liu Y, Zhou H, Ding B, Xu F, Tong H, Deng Z, Hong X, Chem. Sci 2019, 10, 1219. [PubMed: 30774922]

[39]. Zhang XD, Wang H, Antaris AL, Li L, Diao S, Ma R, Nguyen A, Hong G, Ma Z, Wang J, Zhu S, Castellano JM, Wyss-Coray T, Liang Y, Luo J, Dai H, Adv. Mater 2016, 28, 6872. [PubMed: 27253071]

[40]. Yang Q, Hu Z, Zhu S, Ma R, Ma H, Ma Z, Wan H, Zhu T, Jiang Z, Liu W, Jiao L, Sun H, Liang Y, Dai H, J. Am. Chem. Soc 2018, 140, 1715. [PubMed: 29337545]

[41]. Zhu S, Hu Z, Tian R, Yung BC, Yang Q, Zhao S, Kiesewetter DO, Niu G, Sun H, Antaris AL, Chen X, Adv. Mater 2018, 30, 1802546.

[42]. Fang Y, Shang J, Liu D, Shi W, Li X, Ma H, J. Am. Chem. Soc 2020, 142, 15271. [PubMed: 32820908]

[43]. Wu Y, Wang C, Guo J, Carvalho A, Yao Y, Sun P, Fan Q, Biomater. Sci 2020, 8, 4438. [PubMed: 32648882]

[44]. Ma Z, Wan H, Wang W, Zhang X, Uno T, Yang Q, Yue J, Gao H, Zhong Y, Tian Y, Sun Q, Liang Y, Dai H, Nano. Res 2019, 12, 273. [PubMed: 31832124]

[45]. Zhang F, Liu Y, Lei J, Wang S, Ji X, Liu H, Yang Q, Adv. Sci 2019, 6, 1901378.

[46]. Zhang N, Li C, Zhou D, Ding C, Jin Y, Tian Q, Meng X, Pu K, Zhu Y, Acta. Biomater 2018, 70, 227. [PubMed: 29412186]

[47]. a)Li W, McIntyre TM, Silverstein RL, Redox. Biol 2013, 1, 50 [PubMed: 25101237] b)Li W, Nieman M, Sen Gupta A, J. Vis. Exp 2016, 115, 54479.

[48]. a)Lu YM, Huang JY, Wang H, Lou XF, Liao MH, Hong LJ, Tao RR, Ahmed MM, Shan C. l., Wang X. l, Fukunaga K, Du YZ, Han F, Biomaterials. 2014, 35, 530 [PubMed: 24120040] b)Trotman-Lucas M, Kelly ME, Janus J, Gibson CL, J. Vis. Exp 2019, 143, 58191.

[49]. Page MJ, Lourenco AL, David T, LeBeau AM, Cattaruzza F, Castro HC, VanBrocklin HF, Coughlin SR, Craik CS, Nat. Commun 2015, 6, 8448. [PubMed: 26423607]

[50]. a)Nan J, Zhu S, Ye S, Sun W, Yue Y, Tang X, Shi J, Xu X, Zhang J, Yang B, Adv. Mater 2020, 32, 1905927b)Miller BS, Bezinge L, Gliddon HD, Huang D, Dold G, Gray ER, Heaney J,

Dobson PJ, Nastouli E, Morton JJL, McKendry RA, Nature. 2020, 587, 588. [PubMed: 33239800]

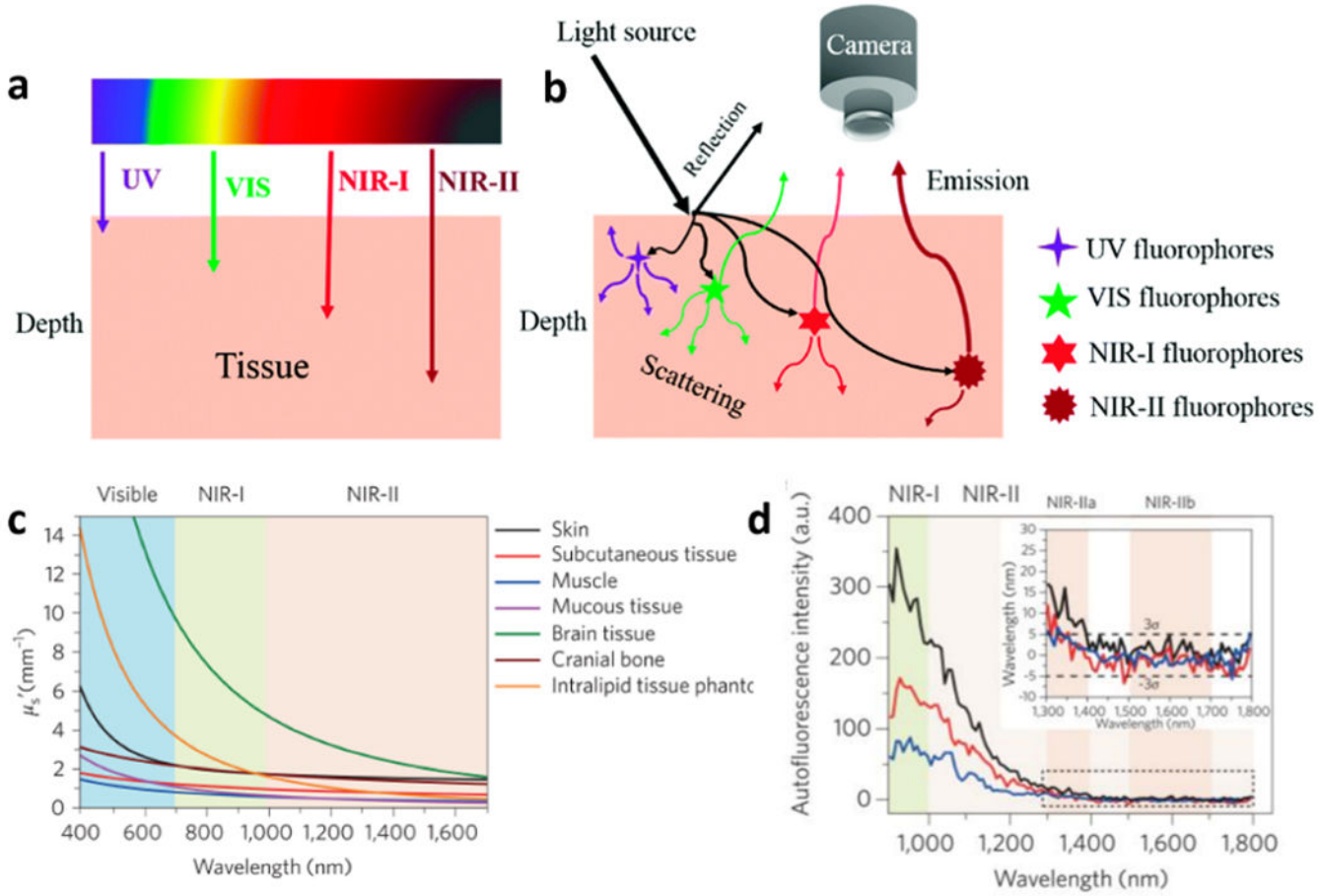

Figure 1.

The interaction between light and biological tissues. a) The tissue penetration depth of light based on different wavelengths. b) The optical characteristic of different wavelength light when peneetrating tissue. NIR-II fluoruorescence emission exhibits the least scattering and greatest penetration depth when compared to UV/VIS and NIR-I fluorescence emission. c) Reduced scattering coefficients of light in different biological tissues and an intralipid tissue phantom as a function of the wavelength within the 400-1700 nm region. d) Autofluorescence spectra of *ex vivo* mouse liver (black), spleen (red) and heart tissue (blue) under 808 nm excitating light, which reveals lowest autofluorescence in the region from 1500 nm to 1800 nm. Inset: Autofluorescence spectra at 1300-1800 nm. a-b) Reproduced with permission.[10] Copyright 2018, Royal Society of Chemistry. c-d) Reproduced with permission.[11a] Copyright 2017, Springer Nature.

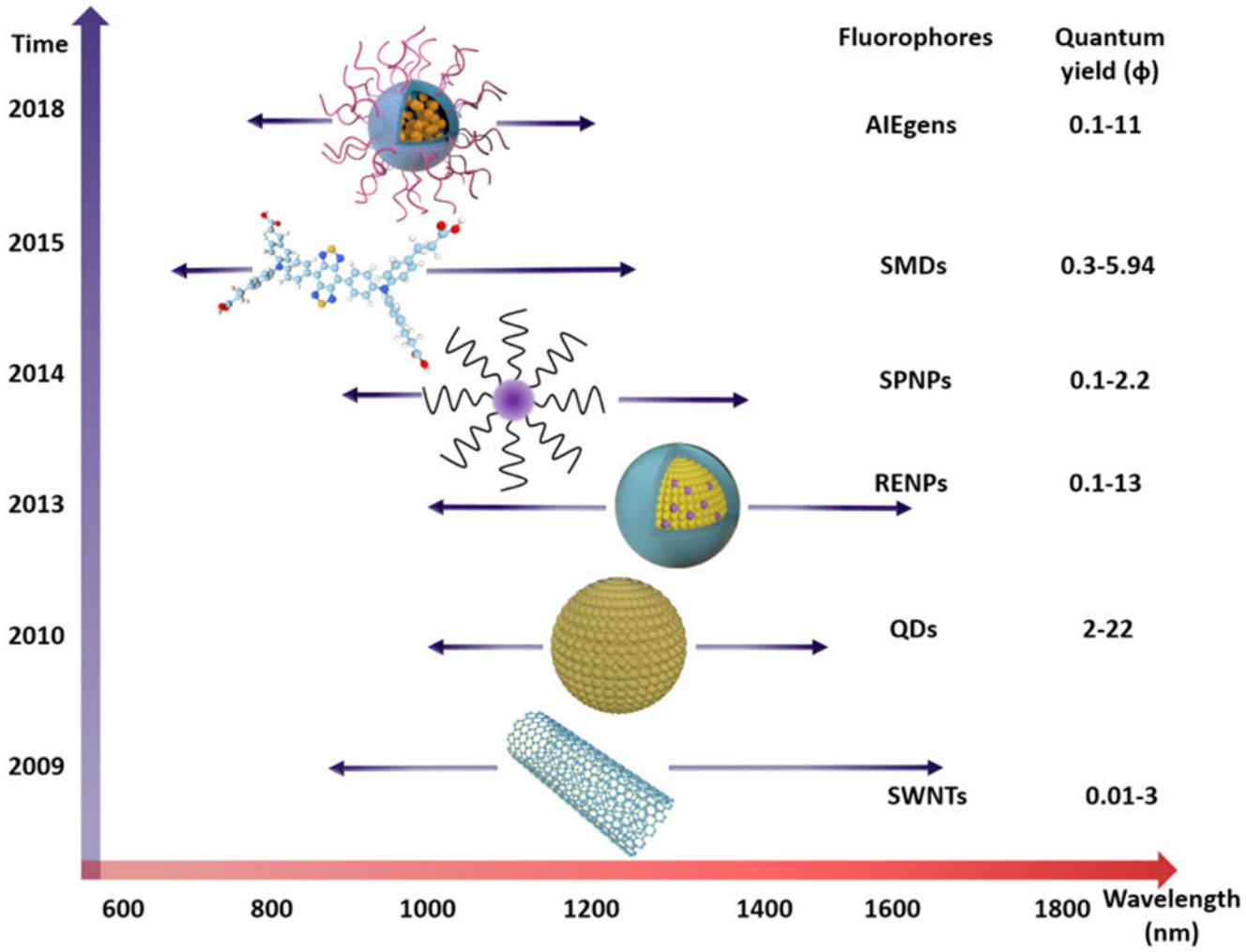

Figure 2.

Representative fluorescent material classes and their optical performance (emission wavelength and quantum yield), including SWCNTs, QDs, RENPs, SPNPs, SMDs, and AIEgens.

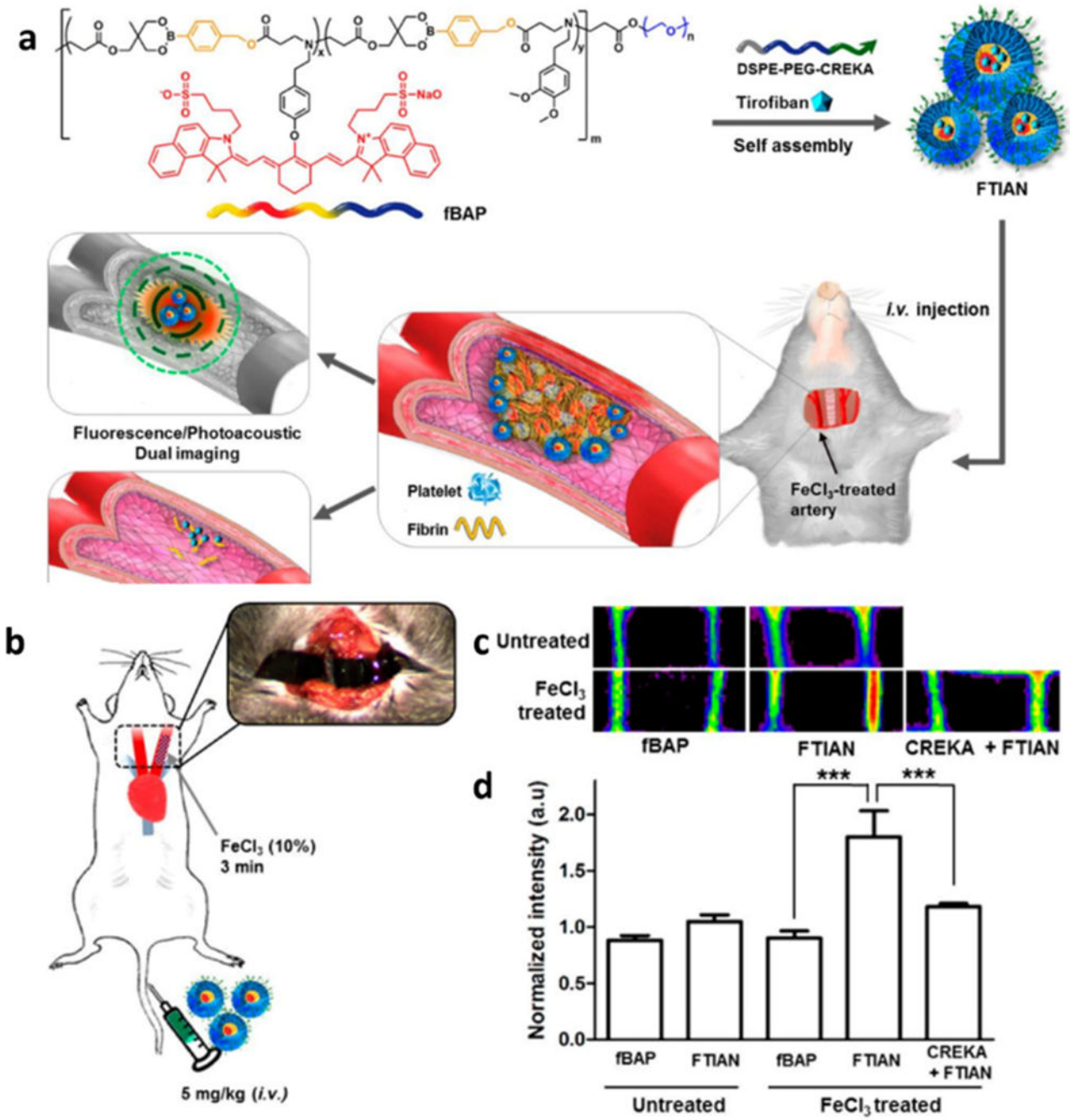

Figure 3.

The multifunational theranostic nano-medicines for thrombus treatment. a) Thrombus-specific FTIAN nano-medicines for NIR-I fluorescence imaging and therapy. b) Scheme representation of $FeCl_3$-induced carotid arterial thrombosis model. c) Directed fluorescent images of the carotid arteries. In each panel, the right is thrombotic artery and the left is the non-injured artery and. d) Normalized fluorescence intensity of thrombus formation in the carotid arteries. Reproduced with permission.[23a] Copyright 2017, American Chemical Society.

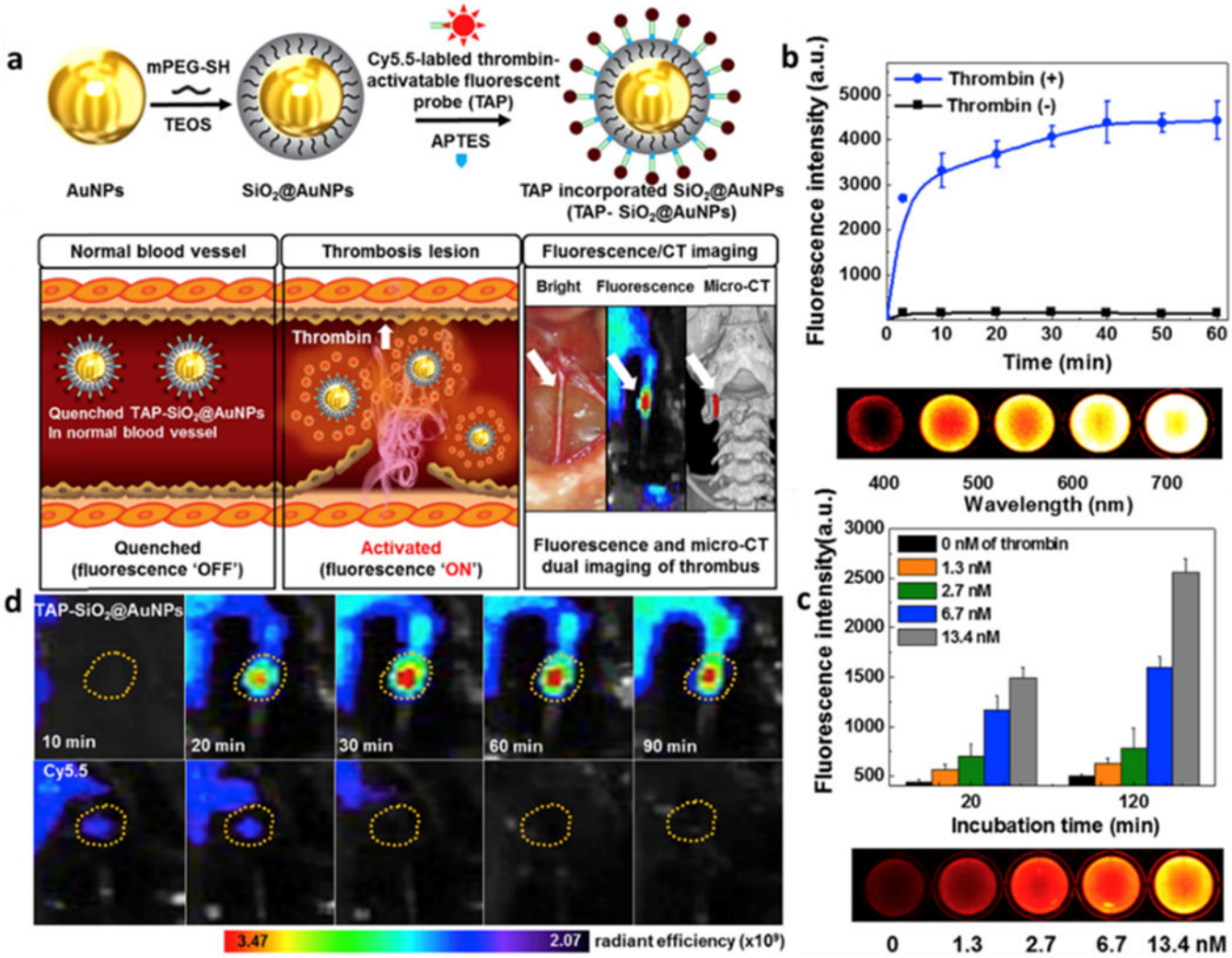

Figure 4.

Responsive nanoparticles for thrombus detection. a) Preparation procedure of TAP-SiO_2@AuNPs, their thrombin-activable NIR fluorescence, and the micro-CT imaging. b) Time-dependent NIR fluorescence activated by thrombin and well plate NIR fluorescence image of TAP-SiO_2@AuNPs with 13.4 nM of thrombin. c) Thrombin concentration-dependent NIRF activation and accordingly 96-well plate NIRF image. d) Time-dependent NIR fluorescence images of *in situ* thrombus formation treated with TAP-SiO_2@AuNPs or Cy5.5 alone. The yellow circles indicate thrombus formation site. Reproduced with permission.[23b] Copyright 2018, Elsevier.

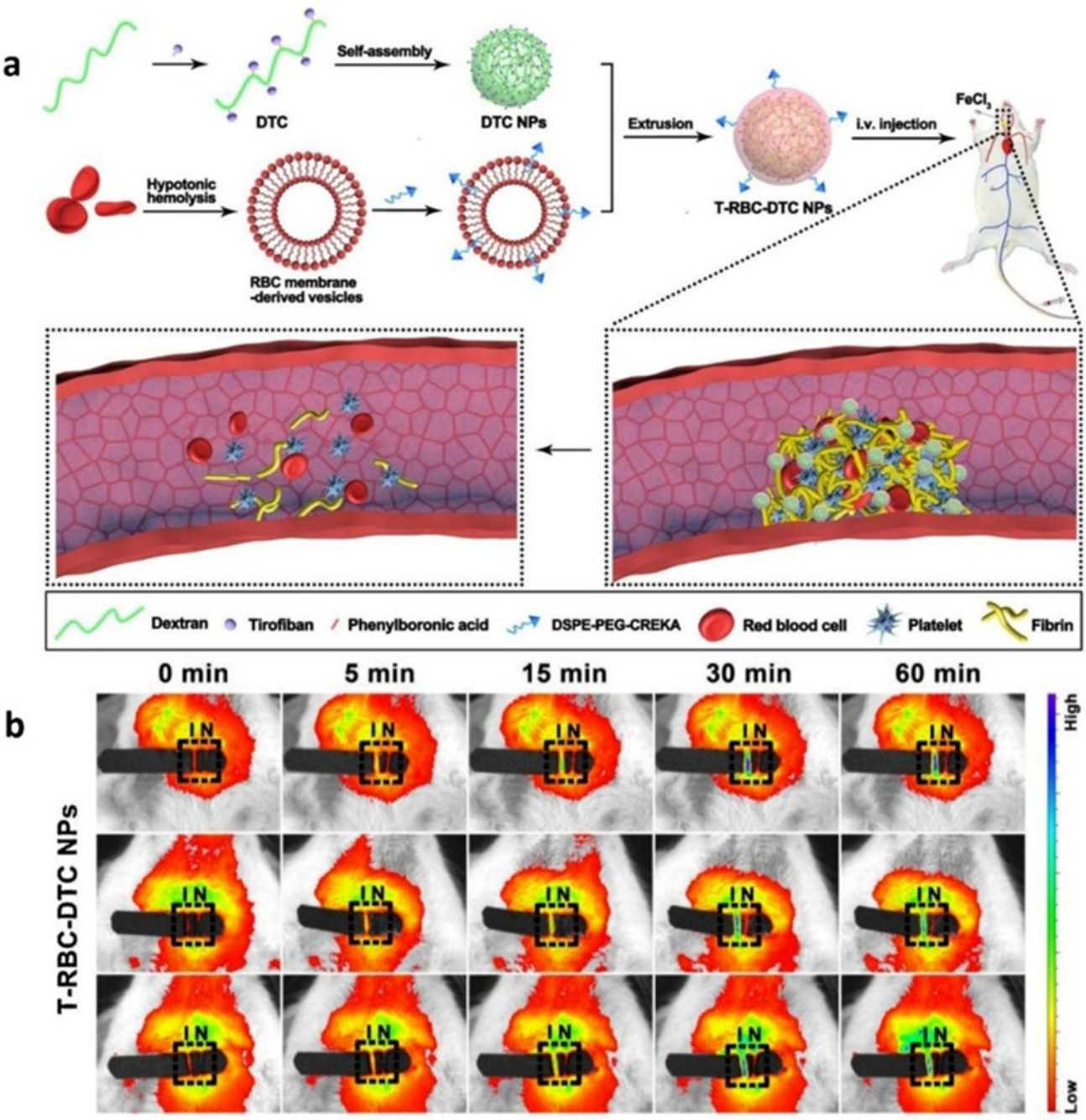

Figure 5.

Biomimetic nanoparticles for targeted treatment of carotid thrombosis. a) Scheme representation of the T-RBC-DTC NPs for highly-effective thrombolysis, and b) *In vivo* fluorescence images of the carotid arteries by Cy5.5 emitted in the NIR-I window, respectively. I and N represent the injured and non-injured artery, respectively (outlined by the black rectangle). Reproduced with permission.[27a] Copyright 2020, Elsevier.

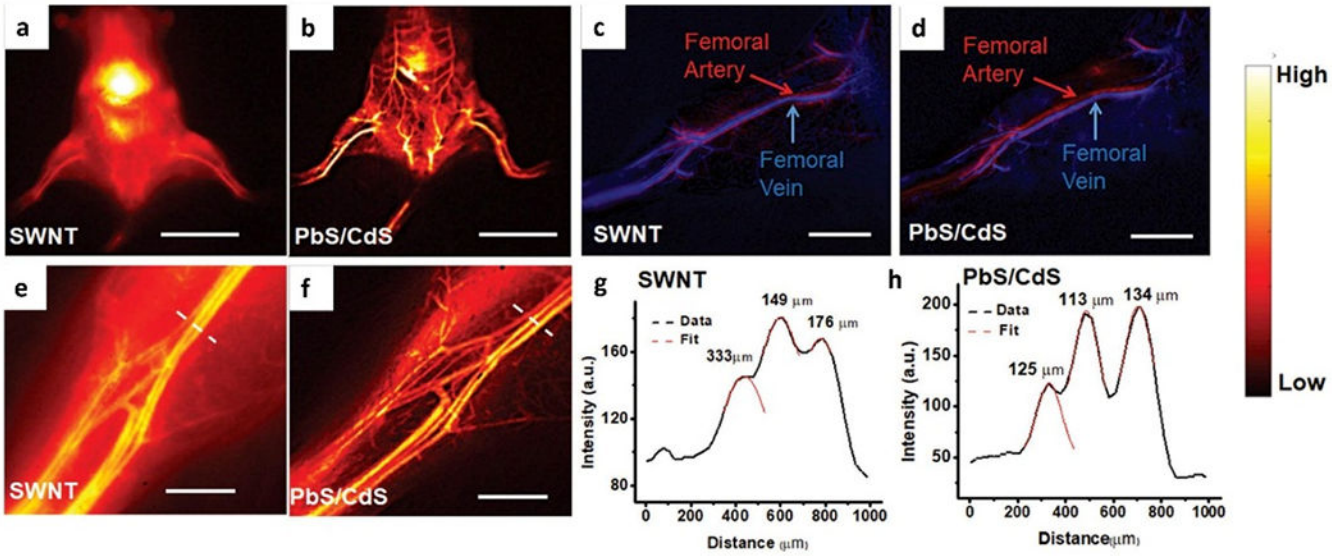

Figure 6.

Whole body and vascular imaging in NIR-II optical window by using SWNT and PbS/CdS NIR-II fluorophores. a, b) Whole body NIR-II fluorescence imaging after tail-vein injection of (a) SWNTs and (b) PbS/CdS. c, d) Unambiguous imaging of femoral artery and vein after tail-vein injection of (c) SWNTs and (d) PbS/CdS. e, f) High-magnification images of the hindlimb vasculature imaged by (e) SWNTs and (f) PbS/CdS. g, h) Representative cross-sectional fluorescence intensity profiles of (e) SWNTs and (f) PbS/CdS. e, f) Gaussian fits to the profiles are shown in red dashed curves. Scale bar: 2 cm (a, b), 5 mm (c, d), 2 mm (e, f). Reproduced with permission.[30] Copyright 2018, John Wiley and Sons.

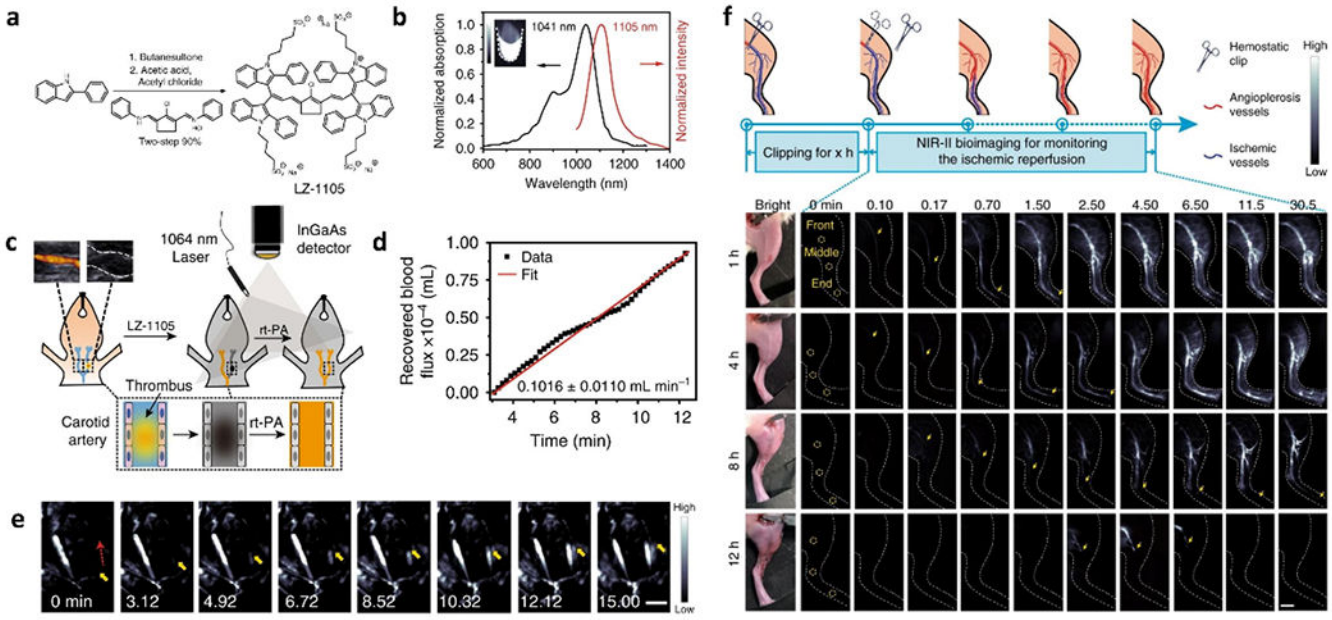

Figure 7.

Various vessel behaviors imaging by SMDs. a) Synthetic route of LZ-1105. b) Optical performance of LZ-1105 in PBS, which exhibits peak adsorption at 1041 nm and peak emission at 1105 nm. Inset: NIR-II fluorescence image of LZ-1105 (10 μM) in PBS. c) Schematic illustration of the thrombolysis process. d) Recovered blood flux during thrombolysis process as a function of time. e) Real-time NIR-II images of the carotid artery. f) Schematic illustration of real-time detection the ischemic reperfusion process by LZ-1105 after various period clipping treatment (1400 nm long-pass, λ_{ex} = 1064 nm, 300 ms) as indicated. Reproduced with permission.[28] Copyright 2020, Springer Nature.

Table 1.

The NIR-II fluorophores for vascular behavior imaging.

Type	NIR-II Fluorophores	Excitation wavelength (nm)	Emission wavelength (nm)	QY (%)	Applications	Refs
SWCNTs	SWCNTs-cholate	808	900-1500	0.4	Tumor vessels imaging	[12a]
	SWCNTs-IRDye800	785/808	1100-1400	—	Hindlimb vessels imaging	[31]
	LV SWNTs	808	1500-1700	0.01	Cerebrovasculature, Hindlimb vessels imaging	[32]
RENPs	NaYbF4:Er/Ce@NaYF4	980	1550	0.27-2.73	Cerebral vascular imaging	[14c]
	$NaErF_4@NaYF_4$	808	1525	—	Cerebral vascular imaging	[33]
QDs	PbS/CdS	808	1600	2-20	Hindlimb vessels imaging Hemodynamics	[30]
	$CulnSe_2/ZnS$	808	920-1224	21.8	Tumor vessels imaging	[34]
SPNPs	PBT	980	1156	0.1	Cerebral vasculature imaging, hemodynamics	[35]
	pDA	808	1047	1.7	Ultrafast NIR-II imaging of arterial blood flow	[15a]
	PTQ	980	1057	1.25	Cerebral ischemic stroke imaging	[36]
AIEs	2TT-oC6B	808	1030	11	Hindlimb vessels imaging Brain inflammation imaging	[37]
	HLZ-BTED	808	1034	0.18	Tumor blood vessels imaging	[38]
SMDsA	CH1055-PEG	808	1055	0.3	Lymphatic vasculature imaging	[16a]
	IR-EI	808	1071	0.7	Brain vessels imaging	[39]
	IR-FTAP	808	1048	5.3	Hindlimb vessels imaging	[40]
	FD1080	1064	1080	0.31	Vessels imaging	[16c]
	CH4T		1055	1.08	Vessels imaging	[16d]
	Commercial cyanine dyes	808	NIR-II tail emission	—	Brain and hindlimb vessel imaging	[16e, 41]
	FM1210	980	1210	0.036	Abdominal/femoral vascular imaging	[42]
	LZ1105	1064	1105	1.69	Hindlimb vessel imaging Monitoring carotid artery thrombolysis/Ischemic reperfusion.	[28]

Table 2.

The representative mouse thrombosis model and accordingly theranostic systems.

Thrombosis model	Nanosystems	Function and application	Refs
$FeCl_3$-induced carotid thrombosis mouse model	FTIAN NPs	Fibrin-targeted, H_2O_2-responsive. Thrombolytic imaging. Prevention thrombus formation.	[23a]
$FeCl_3$-induced *in-situ* thrombotic model	TAP-SiO_2@Au NPs	Thrombin-activatable fluorescence Dual modalities (CT/NIRF) for thrombus imaging	[23b]
$FeCl_3$-induced carotid artery thrombosis model	T-RBC-DTC NPs	H_2O_2-responsive, targeted antithrombotic drugs delivery. Thrombolytic imaging.	[27a]
Pulmonary embolism mouse model Mesenteric arterial mouse model Ischemic stroke mouse model	PNP-PA NPs	Targeted thrombolytic drugs delivery Low bleeding risk	[27b]
In vitro artificial thrombus model Simulated vein vasculature model Celiac vein thrombus mouse model	MMNM/PM nanomotors	Targeted thrombolytic and anticoagulant drugs delivery. Deep thrombus penetration depth by NIR irradiation.	[25]
Middle cerebral artery occlusion (tMCAO) mouse model	Microthrombus-targeting micelles	Reactive oxygen species (ROS) responsive. Enhanced neuroprotection and blood perfusion.	[29b]
In vitro artificial thrombus model $FeCl_3$ induced lower limb thrombosis model	Carbon nanospheres	Photothermal/photodynamic thrombosis therapy.	[45]
$FeCl_3$-induced mouse mesenteric vessel thrombosis model. Tail bleeding model *In vitro* capillary thrombus model	cRGD functionalized liposomes	Highly-effective thrombolysis	[46]